Journal of Materials Science and Chemical Engineering, 2026, 14(2), 73-89
https://www.scirp.org/journal/msce
ISSN Online: 2327-6053
ISSN Print: 2327-6045

Comprehensive Study of the Effect of Hematite-Rich Sludge from Water Treatment Station on the Physical Properties of Metakaolin-Based Geopolymer Cements

Gustave Tchanang[1,2*], Jean Marie Kepdieu[2], Berthelot Sop Tamo[3], Kalaya Goumou[1], Ansoumane Keita[1], Isaï Haba[1], Mamadou Yaya Baldé[2,4], Line Carrel Dassi Meka[2], Cyprien Joel Ekani[2], Chantale Njiomou Djangang[2*], Phillipe Blanchart[5]

[1]Department of Chemistry, University Julius Nyerere of Kankan, Kankan, Guinea
[2]Department of Inorganic Chemistry, University of Yaoundé I, Yaoundé, Cameroon
[3]School of Geology and Mining Engineering, University of Ngaoundéré, Meiganga, Cameroon
[4]Department of Chemistry, University Gamal Abdel Nasser of Conakry, Conakry, Guinea
[5]Unité Mixte de Recherche 7315, Institut de Recherche sur les Céramiques, Centre National de la Recherche Scientifique, University of Limoges, Limoges, France
Email: *tchanang.gustave@yahoo.com, *chantale.njiomou@facsciences-uy1.cm

How to cite this paper: Tchanang, G., Kepdieu, J.M., Tamo, B.S., Goumou, K., Keita, A., Haba, I., Baldé, M.Y., Meka, L.C.D., Ekani, C.J., Djangang, C.N. and Blanchart, P. (2026) Comprehensive Study of the Effect of Hematite-Rich Sludge from Water Treatment Station on the Physical Properties of Metakaolin-Based Geopolymer Cements. *Journal of Materials Science and Chemical Engineering*, **14**, 73-89.
https://doi.org/10.4236/msce.2026.142005

Received: January 7, 2026
Accepted: February 21, 2026
Published: February 24, 2026

Abstract

This work aimed to study the effect of WTHs (Water treatment hematite-rich sludge) additives on the properties of geopolymers cement. Three formulations of geopolymer cement based on metakaolin powder substituted with 0, 5 and 10 wt.% of WTHs were investigated and the obtained pastes were characterized after curing times varying from 7 to 28 days. X-ray diffraction (XRD) and FT-IR patterns of metakaolin and WTHs dry powders indicate that they were in the amorphous states with illite, lepidocrocite and quartz in low concentrations in metakaolin and mainly hematite in the sludge. The pastes demonstrated an accelerating effect of the WTHs. The specimens showed weak linear shrinkage that increased slightly with sludge additive (from 0.5% to 1.7%). Improved apparent density was obtained with increasing WTHs contents (1.83 to 1.97 g/cm^3). The Porosity was improved for 5% WTHs (67% to 77%) with a slight drop for 10%. The optical microstructure exhibits pores interconnectivity with appearance of some macropores favoured by WTHs additives that promoted a three-dimensional porous structure. The products exhibited a compressive strength of 14 MPa on day 28 and could be used as structural and porous materials required for thermal and acoustic isolation.

Keywords

Geopolymer Cements, Hematite-Rich Sludge, Porosity, Linear Shrinkage, Apparent Density

1. Introduction

Sustainable development is a topic of global interest. Building and construction sector is one of the most critical sector responsible for approximately 40% of CO_2 emissions worldwide [1]. The massive use of ordinary Portland cement is considered to be environmentally unfriendly given the quantity of CO_2 produced and energy consumed during the manufacturing process. To reduce the carbon footprint related to cement industries, research to produce ecological alternatives for conventional cement is urgent. In that spirit, Joseph Davidovits introduced geopolymers as a family of less-polluting mineral binders [2]. Indeed, they are synthetic alkali-activated aluminosilicate materials produced from the reaction of an aluminosilicate precursor with a highly concentrated aqueous alkali hydroxide or silicate solution [3]. They have been found to provide comparable performances to traditional cementitious binders, but with significantly reduced greenhouse gas emissions and also economic reasons [4] [5]. Their successful utilization in many fields such as thermal insulators, high-tech ceramic and fire-resistant materials, protective coatings, refractory adhesives has made them become challenging materials of high interest and common raw materials used are volcanic slag, pozzolan, aluminosilicates as metakaolin and some industrial wastes [6] [7]. Various additives are also considered with the aim of improving the properties of the products and broadening the areas of application [7]. On that line, the use of low-cost and less polluting materials and methods by many workers today make the geopolymerization process to be more economically and environmentally valuable [7] [8]. Hematite and red sludge hematite rich-laterites mixed to metakaolin or fly ashes have been used in geopolymerization and the obtained results reveal that all were favourable to efficient mechanical properties regardless of the alkaline activating solution used [9]-[11]. Nevertheless, the studies on iron based geopolymer are still limited as the current research and development of geopolymer usually focussing on high silica and alumina based geopolymer due to its high resistance against temperature and high durability. Water treatment hematite-rich sludge (WTHS) are of little-known applications so far. However, it has been found to be Si/Al-rich materials and have been tested in geopolymer formulation with success [12]. WTHs are abundant low-cost materials and also of variable compositions depending on their sources. Further understanding is needed regarding the effect of hematite contents of such wastes in geopolymer and evaluate their potential to be used as precursors to make binders for stabilized and compressed blocks.

2. Materials and Experimental Procedures

2.1. Materials and Sampling

The Water treatment hematite-rich sludge (WTHs) is collected from Camwater Co. Cameroon. The kaolin is from Kribi, locality of South Cameroon. The sludge is left to settle for 24 hours in a plastic container, then dried in open air (24˚C ± 3˚C), crushed and sieved to a particle size of 75 µm. Meanwhile, the kaolinitic clay was enriched in clay fraction by wet sieving to pass through a 75 µm mesh and then dried in an oven for 24 hours at 105˚C. The dry product obtained is heated in an electric furnace of type NGS-SRL for 4 hours at 700˚C with a temperature rate of 5˚/min. The thermal treatment allowed the kaolin to be transformed into metakaolin which is more amorphous and reactive [4] [13]. The activating solution was prepared by mixing equal volumes of the aqueous solution of sodium hydroxide (8M) and sodium silicate (SiO_2: 28.7%; Na_2O: 8.9% and H_2O: 62.4%).

2.2. Preparation of Geopolymers Cement Pastes

The formulation of geopolymer cement is made by mixing metakaolin, the WTHs powder and activating solution in the ratios shown in Table 1. The ratio is selected as the best consistency after several tests using the Vicat apparatus. Three formulations are then retained; the first one, labelled MKS0 was made by mixing only the solid precursor, namely metakaolin with the activator solution and was used as reference cement. Two other formulations where 5% and 10% by mass of metakaolin were substituted with sludge powder and denoted MKS5 and MKS10 were done respectively. Above 10% substitution, the paste loses its homogeneity and is transformed into small agglomerates. The mixture was stirred using an M&O brand mixer, model N50-G until a homogeneous paste is obtained. One part of the fresh paste was used to determine the setting times and the other poured into cylindrical molds (diameters = 20 mm and heights = 40 mm) in PVC for further analyses. After casting, the specimens obtained were covered with a thin polyethylene film then left at room temperature in the laboratory (24˚C ± 3˚C) for 24 hours. The mechanical measurements were carried out on cylindrical specimens on day 28 according to standard EN 196-1 [14] [15].

Table 1. Formulations of geopolymer cement pastes.

Formulation	% MK	% Sludge	L/S
MKS0	100	0	0.8
MKS5	95	5	0.8
MKS10	90	10	0.8

2.3. Technical Characterization

The starting materials (MK and WTHS) were characterized using inductive Couple Plama (ICP) for chemical composition, XRD, amorphous phase content, Humidity and dryness, FTIR spectroscopy for structural composition and the BET

specific surface area (SSA).

Geopolymer cement performance were evaluated via the measurement of the setting time according to the EN 196-3 using the Vicat device [16], linear shrinkage using a digital caliper on cylindrical test discs, Archimedes measure of apparent density and open porosity. The compressive strength is measured according to standard EN 1961 [17] [18]. Optical microscopy was carried out using a Ceramics Instruments Model 101T-M7 optical microscope equipped with a stereomicroscope, a binocular head and a tablet with integrated camera.

3. Results and Discussion

3.1. Characteristics of Starting Materials

The dryness rate and water content of the sludge powder were found to be 93.89% and 6.49% respectively. These results indicate that the sludge used is classified as dry because its dryness is greater than 85% [19].

The chemical composition of metakaolin is given in **Table 2**.

Table 2. Chemical composition of metakaolin.

Oxides	Content (%)
SiO_2	51.46
Al_2O_3	41.71
Fe_2O_3	2.66
CaO	0.10
MgO	<0.01
Na_2O	0.39
K_2O	0.70
TiO_2	0.95
LOI*	2.03
Total	100

*LOI: Loss of Ignition.

Metakaolin is mainly composed of silica (SiO_2) and alumina (Al_2O_3), the main oxides for geopolymerization. The combination of Na_2O and K_2O values suggests the presence of micaceous minerals and feldspars. The data also reveals a low LOI value, which therefore suggests a low quantity of organic matter. The Si/Al molar ratio of 2.1 is in quite good and is in accordance with other work specially that of Fernàndez-Jimènez *et al.* (2005) who demonstrated that an aluminosilicate precursor reacts easily in the presence of an alkaline solution when Si/Al molar ratio is less than 4 [20] [21].

Table 3 presents the values of the specific surface area (SSA) of the starting materials. The specific surface area of MK is greater than that of WTHs powder, which may lead to greater reactivity of the aluminosilicate powder compared to the sludge.

Table 3. SSA values of metakaolin and WTHs.

Raw sample	MK	WTHs
SSA (m^2/g)	47.87	7.82

Figure 1 presents the structural phases of starting kaolin (**Figure 1(a)**) in comparison with those of metakaolin (**Figure 1(b)**).

Figure 1(a) highlights the presence of kaolinite [$Si_2O_5Al_2(OH)_4$], illite [ɤ-FeO(OH)], lepidocrocite [$K_{x+y}[(Si_{4-x}Al_x)O_{10}(Al_{2-y}Fe(II)_Y)(OH)_2]$], and quartz ($SiO_2$). After the amorphization of the clay fraction at 700˚C, the disappearance of the kaolinite was observed (**Figure 1(b)**). The presence of a dome around 2θ =15˚ - 25˚ on the MK curve was also noted, which expressed the existence of an amorphous phase in this material [11]. This amorphous phase is obviously that of metakaolinite following dehydroxylation. This observation corroborates the rate of amorphous phase obtained which is 65.15%. The rate of 50.13% for the sludge evidences that it is mainly made up of amorphous. This is in agreement with the appearance of the diffractogram of **Figure 1(c)** which presents several halos characterizing amorphous phases. The only crystalline phase observed is hematite, a coloring oxide which could explain the reddish color of WTHs.

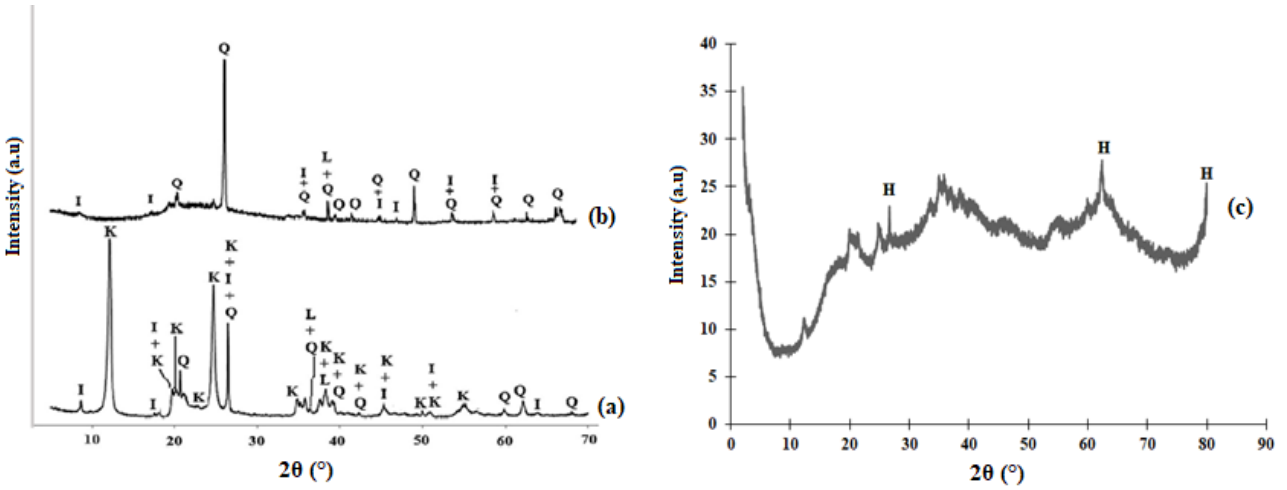

Figure 1. XRD patterns of (a) Kaolin, (b) Metakaolin and (c) WTHs: Kaolinite (K), Illite (I), Lepidocrocite (L), Quartz (Q) and Hematite (H).

Figure 2 presents the FTIR spectrum of the sludge. A broad band is observed at 3288 cm^{-1}, a band not assigned until now. The absorption bands around 1366 - 1603 cm^{-1} are attributed to the stretching vibrations of the C=O, C=C, and C=O groups which belong to organic matter [22]. The band observed at 906 cm^{-1} which expresses the deformation vibration of the Al-OH bonds and that at 999 cm^{-1} which reflects the Si-O-Si bond vibration [23] [24]. Finally, the absorption band at 515 cm^{-1} indicates the vibration of Fe-O attributed to the hematite in accordance with its XRD diffractogram. This high concentration of hematite also explains the strong red color of the WTHs [25] [26].

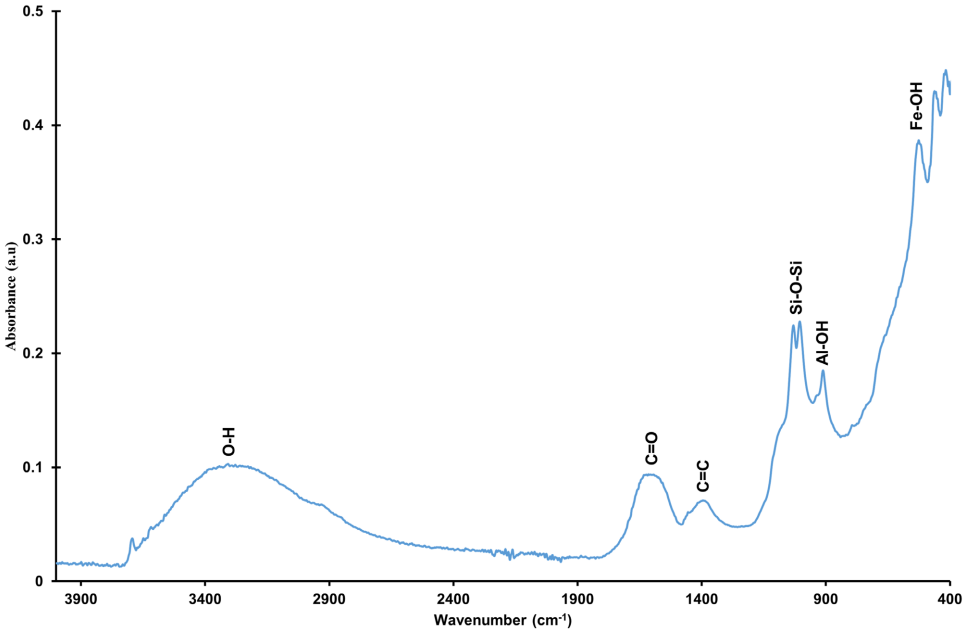

Figure 2. FTIR spectrum of the WTHs.

3.2. Characteristics of Geopolymers Cements

3.2.1. Setting Time

The initial and final setting times shown in **Figure 3** exhibit the decreasing of setting times with increasing WTHS contents from 69 - 105 min for 5% and 58 - 90 min for 10%. The formation of the geopolymer gel strongly depends on the availability of silicates and the aluminates ions which have a tendency to condense to form Si-O-Si and Al-O-Al bonds respectively [27]. The sludge may promote the dissolution of the aluminosilicates and reduce the alkaline cations by entrapping them in the medium. It also promotes the process of polycondensation of the silicate and aluminate monomers, hence the reduction in the setting time. In terms of setting acceleration, the reduction in setting time observed in this study (58 - 90 min for MKS10) aligns with findings by Sekizkades *et al.* (2025) for transition metal oxide-modified geopolymers, where Fe_2O_3 reduced setting times by 40-60%. This setting accelerating effect could be advantageous for numerous applications where the use of the paste requires a reduced setting time for the work.

3.2.2. Fourier Transformed Infrared Spectra

Figure 4 shows the FT-IR spectra of the geopolymer cements. The bands at 3400 - 3450 cm^{-1} and 1640 - 1650 cm^{-1} correspond to deformation vibration of the H-O-H bond and the elongation vibration of the O-H groups respectively [28]. The absorption bands around 976 - 987 cm^{-1} reflect the presence of aluminosilicate gel in the products obtained [24]. The absorption bands around 773 - 776 cm^{-1} correspond to the vibrations of the connections Al(VI)-OH and Al(VI)-O where aluminum in VI coordination. Those around 666 - 692 cm^{-1} express the symmetrical elongation vibration of the Si-O and Al-O bonds, which shows that the aluminum initially in coordination (VI) in metakaolin occupies the coordination (IV) in ge-

opolymers [29]. The shoulder around 547 - 566 cm^{-1} expresses the deformation vibrations of the Si-O-Si and Si-O-Al bonds of the network [24]. Finally, the absorption bands around 408 - 428 cm^{-1} and 382 - 392 cm^{-1}, characteristic of vibrations of Ti-O and Fe-O bonds. No new link was established due to the presence of sludge.

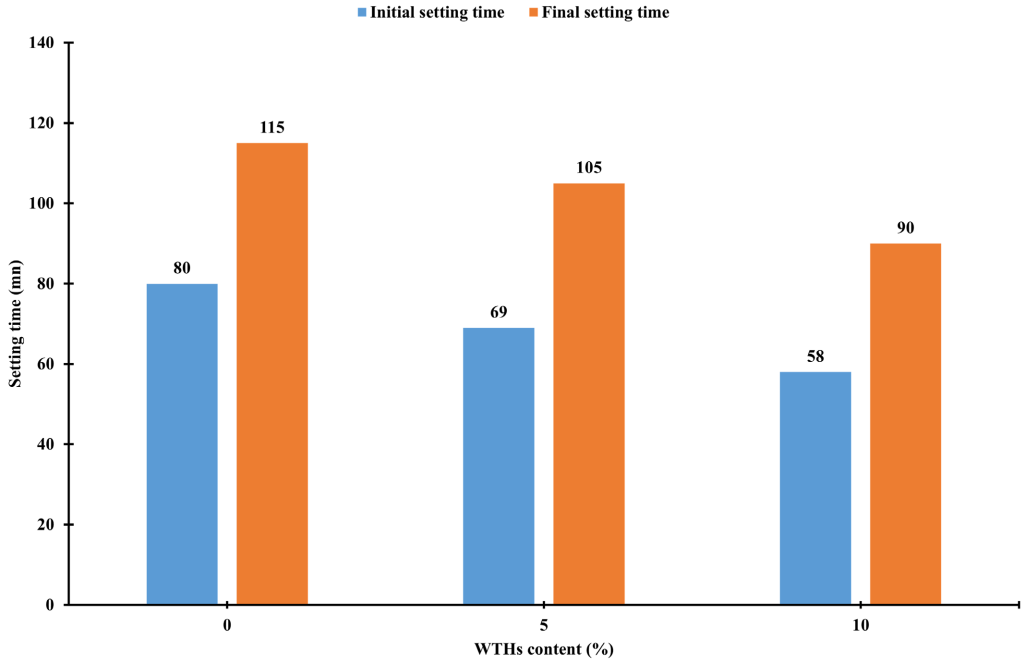

Figure 3. Initial and final setting times.

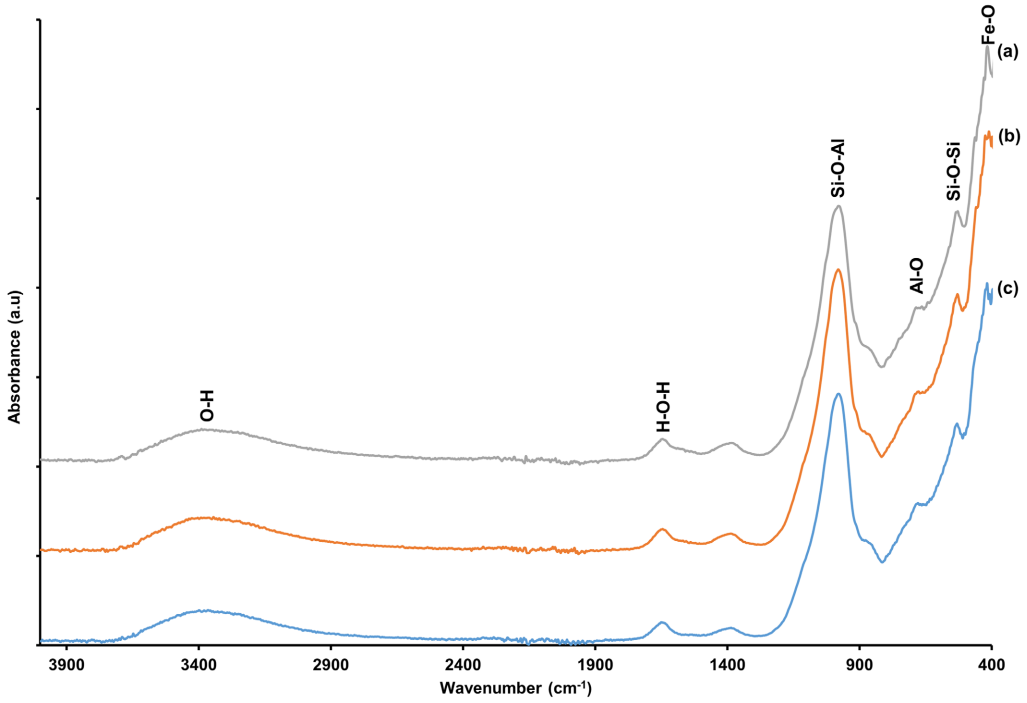

Figure 4. FTIR spectra of (a) MKS0, (b) MKS5 and (c) (MKS10).

3.2.3. Linear Shrinkage

Figure 5 indicates the changes of the linear shrinkage of the geopolymers as a function of age. It increases very slightly with age for formulations without or with 5% sludge and it increases rapidly with the addition of sludge to 10%. In all cases, the linear shrinkage remains very low, 0.5% for MKS0, 0.6% for MKS5 and 1.7% for MKS10. The increase in shrinkage with the addition of sludge is related to its humidity which is a measure of its water retention capacity in its structure. That sludge used is quite high because its water content is 6.5%. In fact, the shrinkage is due to the departure of the moisture water, a physicochemical process of diffusion on the surface leaving voids to be filled, which generates an internal readjustment of the system which evolves towards a more consolidated and stable state. In general, these shrinkages remain relatively within the acceptable limits of dimensional shrinkages for geopolymer binders reported by Elimbi *et al.*, 2011 [4].

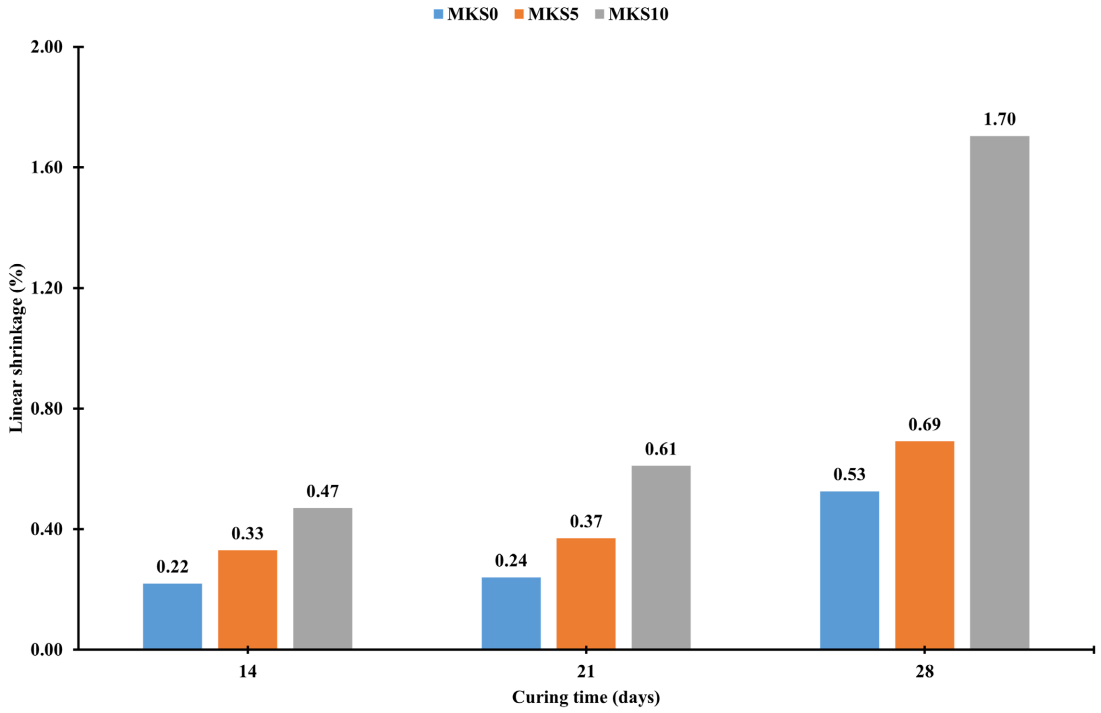

Figure 5. Plots of linear shrinkage versus curing time.

3.2.4. Apparent Density

Figure 6 shows the evolution of the apparent density of the geopolymer specimens as a function of sludge content and curing age. A decrease in apparent density is observed, obviously with age but an increase with the addition of sludge is also observed. This increase is more pronounced on the 21st day: 2.19 g/cm^3 for MKS0, 2.49 g/cm^3 for MKS5 and 2.51 g/cm^3 for MKS10, and on the 28th day: 1.83 g/cm^3 for MKS0, 1.90 g/cm^3 for MKS5 and 1.97 g/cm^3 for MKS10. This means that sludge promotes the densification. Indeed, the sludge seems to promote the agglomeration of particles and their rearrangement which results in a more compact struc-

ture during the geopolymerization process, due to the progressive reduction of water either by its integration into the poly-sialate network or by release due to drying.

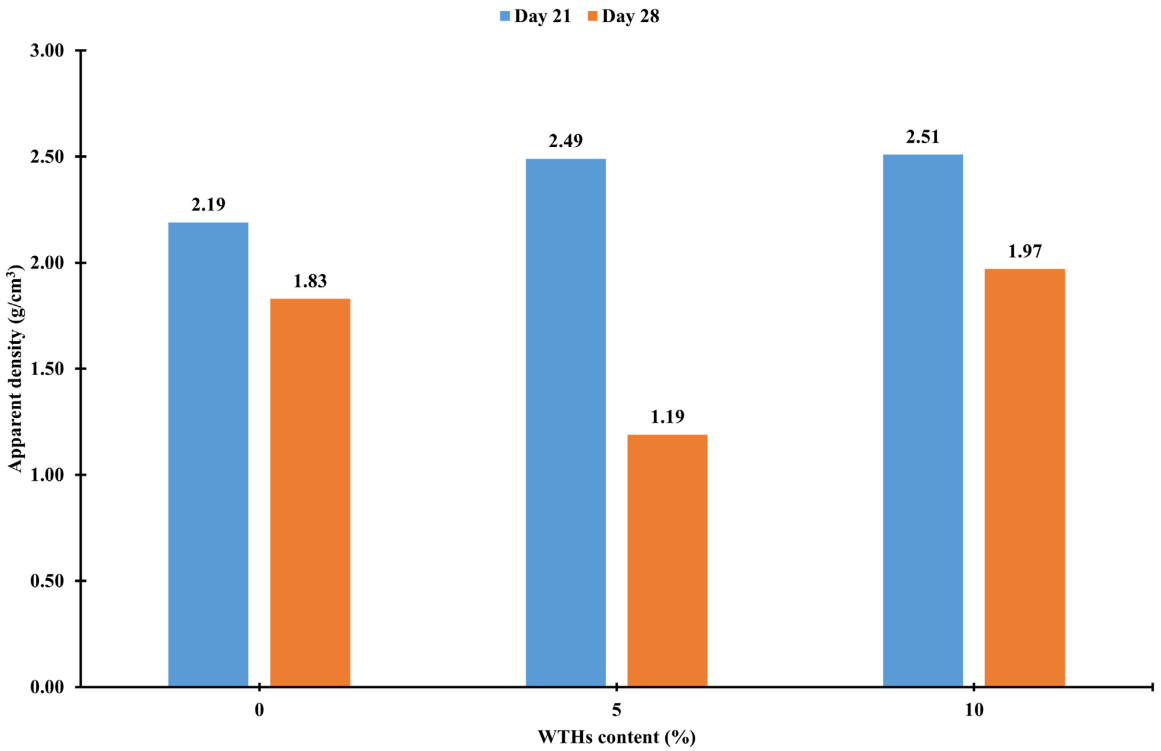

Figure 6. Plots of apparent density versus WTHs content at day 21 and 28.

Figure 7 exhibits the open porosity of the cements as a function of the sludge dosage and curing duration. There is an increase in porosity with increase in sludge. This indicates that sludge, despite its effect of agglomeration and packaging of particles, also promotes the creation of pores. Such a dense structure which integrates pores indicates the presence of a three-dimensional interconnection where the particles in grains are distributed inside the matrix. The whole giving a dense network with pores which are close either to the matrix or to a grain and others which are open [30]-[32]. Obtaining one or the other type of porosity depends on several parameters including the addition of materials such as sludge in the case of geopolymer formulations. In the present work, the sludge used was directly introduced into the geopolymer paste. It has been demonstrated in previous works that this method generates open macroporosity characterized by pronounced interconnectivity.

The porosity-density relationship in this study (1.83 - 1.97 g/cm^3 with 67% - 77% porosity) shows interesting parallels with S. Ma *et al.* (2023) hierarchical porous geopolymers. However, while their systems achieved porosity through templating methods, the WTHs naturally induces interconnected porosity, potentially offering manufacturing advantages.

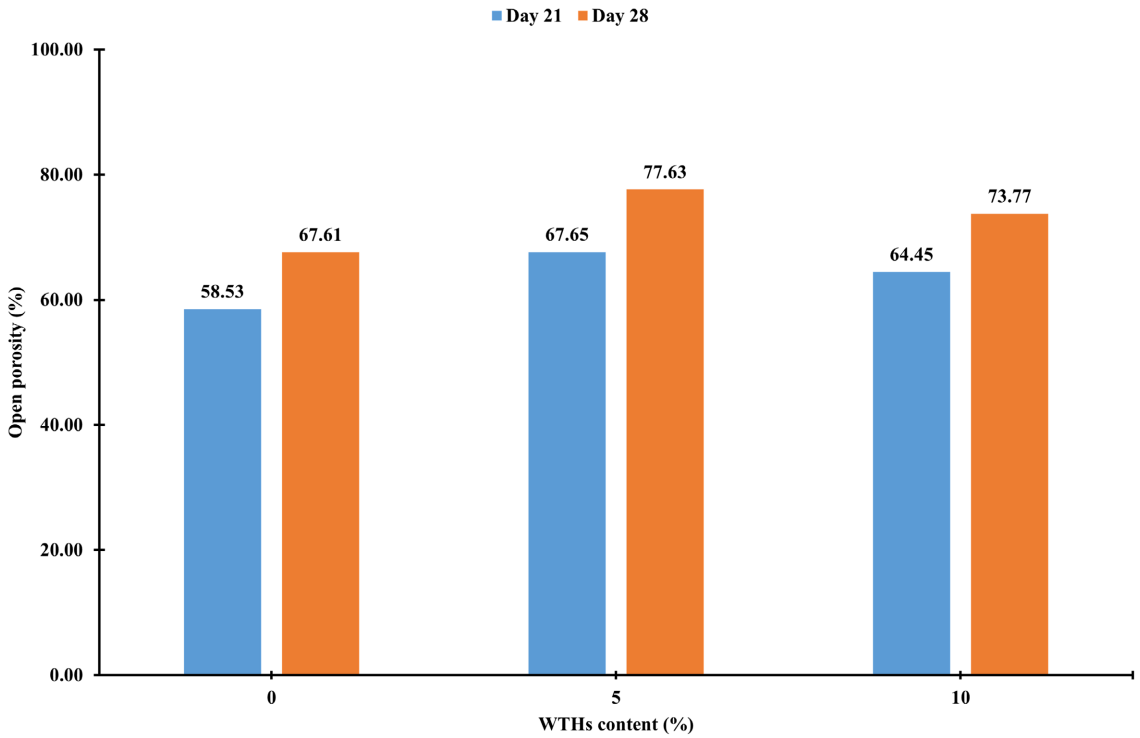

Figure 7. Open porosity at day 21 and 28.

3.2.5. Compressive Strength of Geopolymer Cements

The mechanical resistance of the specimens as a function of the sludge content on the 28th day is shown on **Figure 8**. The compressive strength values obtained (14.36 - 20.04 MPa) are comparable to those reported by G. Liang *et al.* (2022) for lightweight geopolymer foams (8 - 15 MPa) but lower than optimized iron-rich geopolymers such as those by reported by S. Ahmed *et al.* (2020) achieving 25 - 35 MPa with red mud incorporation. This difference can be attributed to the higher porosity (67% - 77%) in our WTHs-modified systems versus 45% - 60% in red mud-geopolymers. Considering those results, the sludge acts globally as a non-reactive filler, but with a noticeable impact on the compressive strength of the geopolymers.

Figure 9 presents the micrographs of MKS0, MKS5 and MKS10. For a magnification of 0.3X, pores are observed in all three geopolymer formulation while for a magnification of 0.7X, pores are observed only in MKS0. This suggests that MKS0 has macropores while MKS5 and MKS10 have micropores. The decrease in pore size of MKS5 and MKS10 could be explained by the addition of sludge which occupies the voids and makes the material dense. Furthermore, it appears that in all cases, the microstructure is more or less homogeneous with a slight difference in the connectivity of the particles in the matrix. Macropores appear on the matrix surface; this observation is correlated with the very high open porosity [33]. This observation confirms the interconnected microstructure which results in a three-dimensional structure, a configuration which is accentuated with the addition of sludge.

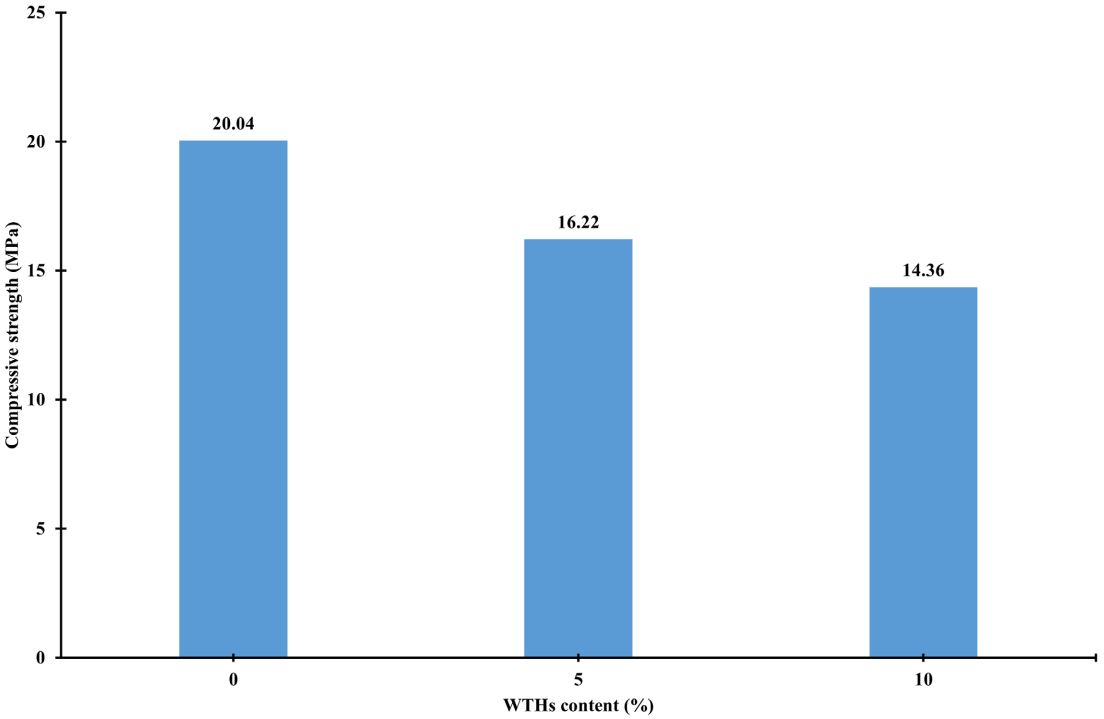

Figure 8. Compressive strength versus WTHs content at day 28.

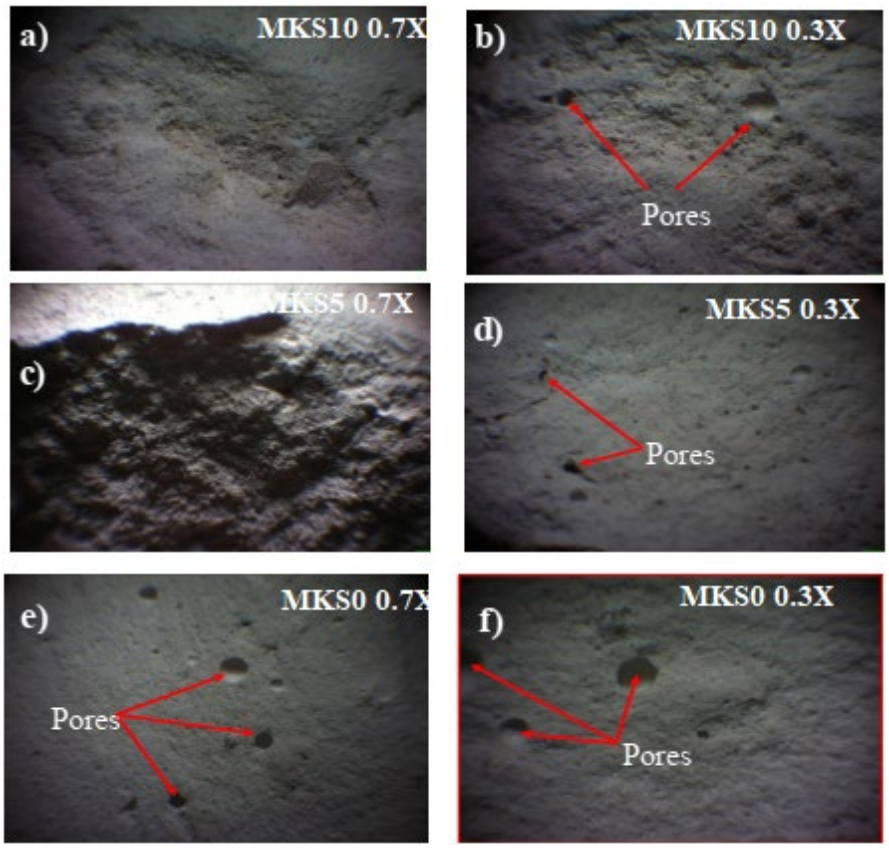

Figure 9. Optical microscopy images of the cement pieces MKS10 ((a) and (b)), MKS5 ((c) and (d)) and MKS0 ((e) and (f)) at 0.7X and 0.3X magnifications.

3.2.6. Physical Appearance

Figure 10 shows the physical appearance of the specimens. MKS0, the specimen with no sludge had pale yellow color while the others are reddish due to the presence of hematite (containing Fe^{3+}) in the sludge.

The sample MKS0 on the 28th day, presented some whitish areas with a saline appearance. This observation is generally due to efflorescence favored by the fairly slow rate of the geopolymerization process [34] [35]. Indeed, when dissolution is slow, CO_2 from the air penetrates the geopolymer matrix and reacts with the alkaline cation to form bicarbonate. The salts formed during efflorescence are generally sodium or potassium bicarbonate or hydroxycarbonate. Regarding the source of K^+ or Na^+ cations, they come from the solid and liquid precursors and constitute the part of the initial mixture which is not involved in the geopolymer gel network. Not only does it reduce the aesthetic appearance but also is a defect for the durability of the product. This phenomenon did not appear on MKS5 and MKS10 formulations which contain the sludge. This is very interesting given the fact that efflorescence is a degrading effect. Considering that sludge contains very little or no sodium ions to create excess of alkaline ions, hence the absence of efflorescence. Therefore, the role of the sludge is highlighted since it changed the typical behavior of aluminosilicate precursors by limiting the excess of ions in the system. The absence of efflorescence in WTHs-containing formulations contrasts with many waste-incorporated geopolymers and suggests that the hematite-rich sludge may act as an alkaline buffer [36], a phenomenon requiring further investigation through leaching studies and pore solution analysis.

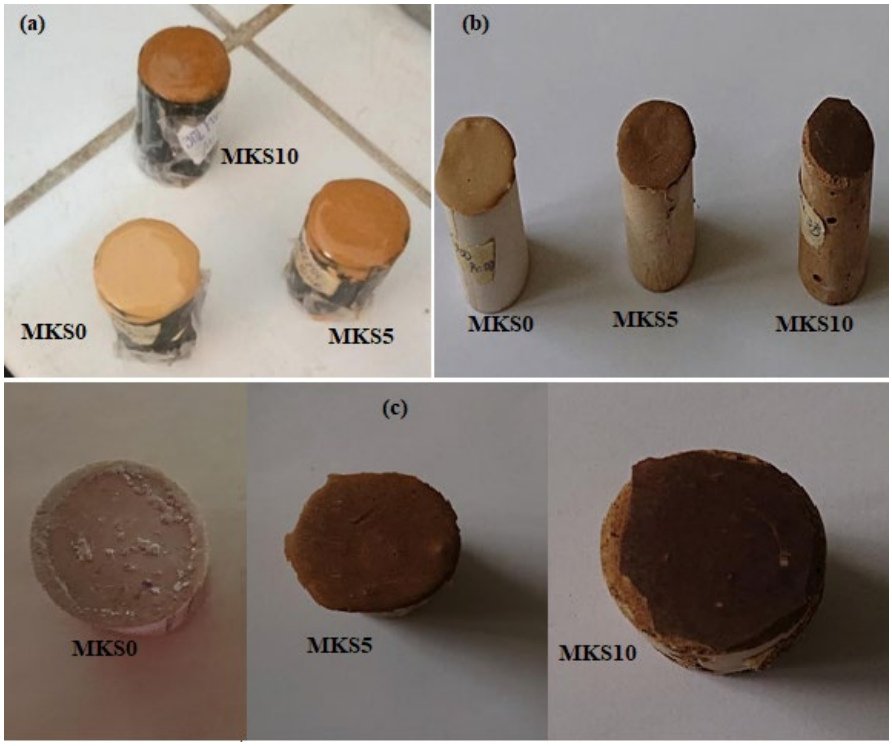

Figure 10. Physical appearances of the samples at (a) day 1 (b) day 7 and (c) day 28.

A Comparison has been done between some properties of the present geopolymer cements and other works in the literature. Table 4 reports the comparison of compressive strength, apparent density, and porosity values with some research works.

Table 4. Comparison of geopolymer cements properties after 28 days.

Geopolymer Cement composition	Compressive strength (Mpa)	Apparent density (g/cm^3)	Related references
metakaolin + hematite rich-sludge	20.04 - 14.36	1.83 - 1.97	Present work
ground granulated blast furnace slag+paper sludge	42		[37]
Fly ash-based geopolymers	16.3 - 47.3	1.36 - 1.86	[38]
Rice husk ash + Blast furnace slag + Metakaolin + aggregate	48	2.070	[39]
Fly ash + Palm oil fuel ash	8.32 - 30.1	1.3 - 1.7	[40]
Class F fly ash + granulated blast furnace slag	3 - 48	0.72 - 1.6	[41]
Ground granulated blast furnace slag-based geopolymers	27 - 39	1.74 - 1.77	[42]
Fly ash and slag	8.5 - 47.50	1.50 - 2.45	[43]

4. Conclusion

Geopolymers cements-based metakaolin and hematite-rich sludge were made with the aim of valorizing the sludge resulting from water treatment. Metakaolin obtained by calcination of kaolin at 700˚C, as a conventional solid precursor, was substituted by 5% and 10% of sludge mass percentages respectively, in the formulation of geopolymer cements and a formulation without 0% sludge was considered as witness. The study measured the initial and final setting times of the cements in the fresh state. Additionally, the physical, mechanical, and microstructural properties of the cement specimens after setting were compared to the reference cement without sludge. The results obtained showed that the sludge has an accelerating effect on the setting. The aluminosilicate/sludge ratio is an important factor to be considered to balance the low toughness of the products. The mechanical resistance on day 28 was around 14 MPa with 10% sludge. The porosity and the apparent density increased with increasing WTHs contents (up to 5% add for porosity) (67% to 77%) and (1.83 to 1.97 g/cm^3) respectively. Sludge makes it possible to obtain cements for structuring and porous materials, favorable for high buildings and thermal insulation. These products can be used when a high porosity and a low density are required, and where a limited mechanical resistance is still acceptable. The geopolymer cements of this study are lightweight cementitious materials due to the presence of the sludge. The latter is also an efficient component due to its high reactivity and availability at a moderate environmental cost. Numerous applications such as thermal and acoustic insulation, high-rise construction, manufacture of membranes for filtration can be well explored beside the well-known properties and advantages of classical geopolymers.

Conflicts of Interest

All authors certify that they have no affiliations with or involvement in any organization or entity with any financial interest or non-financial interest in the subject matter discussed in this manuscript.

Informed Consent Statement

All the authors are voluntarily participating for the submission of this research work.

Consent to Publication

The authors confirm that this manuscript has not been submitted or published previously to any other journal and give full consent for publication of the research work.

Data Availability

The datasets generated during and/or analyzed during the current study are available from the corresponding author on reasonable request.

Authors' Contributions

Gustave Tchanang & Jean Marie Kepdieu: Investigation, Roles/Writing—original draft, Data curation. Njiomou Djangang Chantale: Conceptualization, Methodology; Writing—review & editing, Visualization. Berthelot Sop Tamo, Cyprien Joel Ekani & Phillipe blanchard: Investigation, Writing—review & editing. Mamadou Yaya Baldé, Kalaya Goumou, Ansoumane Keita and Isaï Haba: Writing—review & editing.

References

[1] Lu, W., Tam, V.W.Y., Chen, H. and Du, L. (2020) A Holistic Review of Research on Carbon Emissions of Green Building Construction Industry. *Engineering, Construction and Architectural Management*, **27**, 1065-1092. https://doi.org/10.1108/ecam-06-2019-0283

[2] Davidovits, J. (1989) Geopolymers and Geopolymeric Materials. *Journal of Thermal Analysis*, **35**, 429-441. https://doi.org/10.1007/bf01904446

[3] Ferone, C., Capasso, I., Bonati, A., Roviello, G., Montagnaro, F., Santoro, L., *et al.* (2019) Sustainable Management of Water Potabilization Sludge by Means of Geopolymers Production. *Journal of Cleaner Production*, **229**, 1-9. https://doi.org/10.1016/j.jclepro.2019.04.299

[4] Elimbi, A., Tchakoute, H.K. and Njopwouo, D. (2011) Effects of Calcination Temperature of Kaolinite Clays on the Properties of Geopolymer Cements. *Construction and Building Materials*, **25**, 2805-2812. https://doi.org/10.1016/j.conbuildmat.2010.12.055

[5] Risdanareni, P., Hilmi, A. and Susanto, P.B. (2017). The Effect of Foaming Agent Doses on Lightweight Geopolymer Concrete Metakaolin Based. *AIP Conference Proceedings*, **1835**, Article ID: 020057. https://doi.org/10.1063/1.4983797

[6] Djobo, J.N.Y., Elimbi, A., Tchakouté, H.K. and Kumar, S. (2016) Volcanic Ash-Based Geopolymer Cements/Concretes: The Current State of the Art and Perspectives. *Environmental Science and Pollution Research*, **24**, 4433-4446. https://doi.org/10.1007/s11356-016-8230-8

[7] Ngnintedem, D., Lampe, M., Tchakouté, H. and Rüscher, C. (2022) Effects of Iron Minerals on the Compressive Strengths and Microstructural Properties of Metakaolin-Based Geopolymer Materials. *Gels*, **8**, Article No. 525. https://doi.org/10.3390/gels8080525

[8] Elgarahy, A.M., Maged, A., Eloffy, M.G., Zahran, M., Kharbish, S., Elwakeel, K.Z., *et al*. (2023) Geopolymers as Sustainable Eco-Friendly Materials: Classification, Synthesis Routes, and Applications in Wastewater Treatment. *Separation and Purification Technology*, **324**, Article ID: 124631. https://doi.org/10.1016/j.seppur.2023.124631

[9] Bai, B., Bai, F., Nie, Q. and Jia, X. (2023) A High-Strength Red Mud-Fly Ash Geopolymer and the Implications of Curing Temperature. *Powder Technology*, **416**, Article ID: 118242. https://doi.org/10.1016/j.powtec.2023.118242

[10] Nadia, N.F.J., Gharzouni, A., Nait-Ali, B., Ouamara, L., Ndassa, I.M., Bebga, G., *et al*. (2023) Comparative Study of Laterite and Metakaolin/Hematite-Based Geopolymers: Effect of Iron Source and Alkalization. *Applied Clay Science*, **233**, Article ID: 106824. https://doi.org/10.1016/j.clay.2023.106824

[11] Omar Sore, S., Messan, A., Prud'homme, E., Escadeillas, G. and Tsobnang, F. (2018) Stabilization of Compressed Earth Blocks (CEBs) by Geopolymer Binder Based on Local Materials from Burkina Faso. *Construction and Building Materials*, **165**, 333-345. https://doi.org/10.1016/j.conbuildmat.2018.01.051

[12] Santos, G.Z.B., Melo Filho, J.A., Pinheiro, M. and Manzato, L. (2019) Synthesis of Water Treatment Sludge Ash-Based Geopolymers in an Amazonian Context. *Journal of Environmental Management*, **249**, Article ID: 109328. https://doi.org/10.1016/j.jenvman.2019.109328

[13] Khaled, Z., Mohsen, A., Soltan, A. and Kohail, M. (2023) Optimization of Kaolin into Metakaolin: Calcination Conditions, Mix Design and Curing Temperature to Develop Alkali Activated Binder. *Ain Shams Engineering Journal*, **14**, Article ID: 102142. https://doi.org/10.1016/j.asej.2023.102142

[14] Galobardes, I., Salvador, R.P., Cavalaro, S.H.P., Figueiredo, A. and Goodier, C.I. (2016) Adaptation of the Standard EN 196-1 for Mortar with Accelerator. *Construction and Building Materials*, **127**, 125-136. https://doi.org/10.1016/j.conbuildmat.2016.09.147

[15] Standard, E. (2009) Methods of Testing Cement-Part 1: Determination of Strength. Turkish Standards Institute.

[16] ISO P (2003) 9597, "Méthode d'essai des ciments-Détermination du temps de prise et de la stabilité". P15-473PR et NF EN 193-3, Ciment et Chaux, Afnor Ed.

[17] EN N (2016) 196-1. Méthodes D'essais des Ciments-Partie 1: Détermination des Résistances. AFNOR.

[18] Tebbal, N., Maza, M., Zitouni, S. and Rahmouni, Z.E.A. (2022) Combined Impact of Replacing Dune Sand with Glass Sand and Metal Fibers on Mortar Properties. *Revue des composites et des matériaux avancés*, **32**, 85-90. https://doi.org/10.18280/rcma.320205

[19] Dahhou, M., El Moussaouiti, M., Khachani, N., Assafi, M., Ait Hsain, L., Mostahsine, S., *et al*. (2012) Caractérisation physico-chimique de boues d'unité de production d'eau potable. *MATEC Web of Conferences*, **2**, Article No. 01017. https://doi.org/10.1051/matecconf/20120201017

[20] da Silva Godinho, D.d.S., Pelisser, F. and Bernardin, A.M. (2022) High Temperature Performance of Geopolymers as a Function of the Si/Al Ratio and Alkaline Media. *Materials Letters*, **311**, Article ID: 131625. https://doi.org/10.1016/j.matlet.2021.131625

[21] Fernández-Jiménez, A., Palomo, A. and Criado, M. (2005) Microstructure Development of Alkali-Activated Fly Ash Cement: A Descriptive Model. *Cement and Concrete Research*, **35**, 1204-1209. https://doi.org/10.1016/j.cemconres.2004.08.021

[22] Surekha, G., Krishnaiah, K.V., Ravi, N. and Padma Suvarna, R. (2020) FTIR, Raman and XRD Analysis of Graphene Oxide Films Prepared by Modified Hummers Method. *Journal of Physics*: *Conference Series*, **1495**, Article ID: 012012. https://doi.org/10.1088/1742-6596/1495/1/012012

[23] Liu, J., Deng, X., Ma, Z. and Liu, H. (2023) Effect of Alternative Silicon Sources on Alkali-Activated Carbon Steel Slag Binder and Silicon Sources Substitution Mechanism. *Results in Engineering*, **19**, Article ID: 101322. https://doi.org/10.1016/j.rineng.2023.101322

[24] Torres-Luna, J.A. and Carriazo, J.G. (2019) Porous Aluminosilicic Solids Obtained by Thermal-Acid Modification of a Commercial Kaolinite-Type Natural Clay. *Solid State Sciences*, **88**, 29-35. https://doi.org/10.1016/j.solidstatesciences.2018.12.006

[25] Aliprandi, G., Porfirione, M., Jouenne, C. and Beruto, D. (1996) Matériaux réfractaires et céramiques techniques: Éléments de céramurgie et de technologie. Septima.

[26] Kumar, S., Kumar, A., Malhotra, T. and Verma, S. (2022) Characterization of Structural, Optical and Photocatalytic Properties of Silver Modified Hematite (α-Fe_2O_3) Nanocatalyst. *Journal of Alloys and Compounds*, **904**, Article ID: 164006. https://doi.org/10.1016/j.jallcom.2022.164006

[27] Sekizkardeş, B., Soyer-Uzun, S., Uzun, A., Kuhn, S., Kaya-Özkiper, K. and Kurtoğlu-Öztulum, S.F. (2025) A Comprehensive Review on Red Mud-Based Catalysts: Modification Methods and Applications in Thermal- and Photocatalysis. *ChemCatChem*, **17**, e202401678. https://doi.org/10.1002/cctc.202401678

[28] Mohd Basri, M.S., Mustapha, F., Mazlan, N. and Ishak, M.R. (2021) Rice Husk Ash-Based Geopolymer Binder: Compressive Strength, Optimize Composition, FTIR Spectroscopy, Microstructural, and Potential as Fire-Retardant Material. *Polymers*, **13**, Article No. 4373. https://doi.org/10.3390/polym13244373

[29] Yunsheng, Z., Wei, S. and Zongjin, L. (2010) Composition Design and Microstructural Characterization of Calcined Kaolin-Based Geopolymer Cement. *Applied Clay Science*, **47**, 271-275. https://doi.org/10.1016/j.clay.2009.11.002

[30] Djangang, C., Lecomte, G., Soro, J., *et al* (2010) Properties of Porous Ceramics from Two Cameroonian Clays Mixed with Sawdust: Elaboration de céramiques poreuses à base de sciure de bois et de deux argiles du Cameroun. 1-16.

[31] Ma, S., Yang, H., Fu, S., He, P., Duan, X., Yang, Z., *et al*. (2023) Additive Manufacturing of Geopolymers with Hierarchical Porosity for Highly Efficient Removal of Cs+. *Journal of Hazardous Materials*, **443**, Article ID: 130161. https://doi.org/10.1016/j.jhazmat.2022.130161

[32] Wang, Y. and Abuel-Naga, H. (2025) Unfired Bricks from Wastes: A Review of Stabiliser Technologies, Performance Metrics, and Circular Economy Pathways. *Buildings*, **15**, Article No. 1861. https://doi.org/10.3390/buildings15111861

[33] Riyap, H.I., Bewa, C.N., Banenzoué, C., Tchakouté, H.K., Rüscher, C.H., Kamseu, E., *et al*. (2019) Microstructure and Mechanical, Physical and Structural Properties of Sustainable Lightweight Metakaolin-Based Geopolymer Cements and Mortars Em-

ploying Rice Husk. *Journal of Asian Ceramic Societies*, **7**, 199-212. https://doi.org/10.1080/21870764.2019.1606140

[34] Tan, J., Cai, J., Li, X., Pan, J. and Li, J. (2020) Development of Eco-Friendly Geopolymers with Ground Mixed Recycled Aggregates and Slag. *Journal of Cleaner Production*, **256**, Article ID: 120369. https://doi.org/10.1016/j.jclepro.2020.120369

[35] Tan, J., Cizer, Ö., Vandevyvere, B., De Vlieger, J., Dan, H. and Li, J. (2022) Efflorescence Mitigation in Construction and Demolition Waste (CDW) Based Geopolymer. *Journal of Building Engineering*, **58**, Article ID: 105001. https://doi.org/10.1016/j.jobe.2022.105001

[36] Wang, D., Ma, B., Pang, L. and Wang, Q. (2024) Alkali-Activated Blast Furnace Ferronickel Slag for Cr Immobilization. *Cement and Concrete Composites*, **150**, Article ID: 105560. https://doi.org/10.1016/j.cemconcomp.2024.105560

[37] Adesanya, E., Ohenoja, K., Luukkonen, T., Kinnunen, P. and Illikainen, M. (2018) One-Part Geopolymer Cement from Slag and Pretreated Paper Sludge. *Journal of Cleaner Production*, **185**, 168-175. https://doi.org/10.1016/j.jclepro.2018.03.007

[38] Öz, H.Ö., Doğan-Sağlamtimur, N., Bilgil, A., Tamer, A. and Günaydin, K. (2021) Process Development of Fly Ash-Based Geopolymer Mortars in View of the Mechanical Characteristics. *Materials*, **14**, Article No. 2935. https://doi.org/10.3390/ma14112935

[39] Kabir, S.M.A., Alengaram, U.J., Jumaat, M.Z., Yusoff, S., Sharmin, A. and Bashar, I.I. (2017) Performance Evaluation and Some Durability Characteristics of Environmental Friendly Palm Oil Clinker Based Geopolymer Concrete. *Journal of Cleaner Production*, **161**, 477-492. https://doi.org/10.1016/j.jclepro.2017.05.002

[40] Liu, M.Y.J., Alengaram, U.J., Jumaat, M.Z. and Mo, K.H. (2014) Evaluation of Thermal Conductivity, Mechanical and Transport Properties of Lightweight Aggregate Foamed Geopolymer Concrete. *Energy and Buildings*, **72**, 238-245. https://doi.org/10.1016/j.enbuild.2013.12.029

[41] Zhang, Z., Provis, J.L., Reid, A. and Wang, H. (2015) Mechanical, Thermal Insulation, Thermal Resistance and Acoustic Absorption Properties of Geopolymer Foam Concrete. *Cement and Concrete Composites*, **62**, 97-105. https://doi.org/10.1016/j.cemconcomp.2015.03.013

[42] Alnahhal, A.M., Alengaram, U.J., Ibrahim, M.S.I., Yusoff, S., Metselaar, H.S.C. and Gabriela Johnson, P. (2022) Synthesis of Ternary Binders and Sand-Binder Ratio on the Mechanical and Microstructural Properties of Geopolymer Foamed Concrete. *Construction and Building Materials*, **349**, Article ID: 128682. https://doi.org/10.1016/j.conbuildmat.2022.128682

[43] Mahmoud, H.A., Tawfik, T.A., Abd El-razik, M.M. and Faried, A.S. (2023) Mechanical and Acoustic Absorption Properties of Lightweight Fly Ash/Slag-Based Geopolymer Concrete with Various Aggregates. *Ceramics International*, **49**, 21142-21154. https://doi.org/10.1016/j.ceramint.2023.03.244